

# Estimation of Degradation-Based Reliability in Outdoor Environments

Victor Chan and William Q. Meeker

Department of Statistics

Iowa State University

Ames, IA 50011

July 19, 2001

## **Abstract**

Some important reliability problems involve estimating a life distribution when failure is due to chemical degradation of materials or products that are exposed to the outdoor environment. There is a growing need to obtain timely predictions of such degradation behaviors on the basis of accelerated laboratory tests. Laboratory life tests provide information about degradation processes. Historical weather data are used to characterize the stochastic outdoor environment over time. A physical/chemical model for degradation rate is used as a basis for using these data to produce reliability estimates. We propose and illustrate the use of an evaluation/estimation method that involves time series modeling. The method is illustrated with an example involving the degradation of a solar-reflector material. We will also show how to construct approximate confidence intervals for important reliability metrics.

**Key words:** Service Life Prediction, Time Series, Accelerated Testing, Risk Assessment.

# 1 Introduction

## 1.1 Motivation

Some important reliability applications involve quantifying the service life of materials and products that are subjected to highly variable environmental variables like outdoor temperature or solar radiation. The physical state or performance of these products can often be characterized or measured as a function of time. In other words, it is possible to measure the physical degradation or wear-and-tear of the products as they age and move toward eventual failure. Examples of such products include automotive paints and coatings, whose failure is caused by degradation related to long-term weathering (i.e., exposure to outdoor environmental elements). Common measures of degradation for paints and coatings include gloss loss and color change.

Conventional methodologies for the service life prediction of paint and coating products have, for the past 80 years, typically relied on accelerated outdoor tests (Pearce et al.,1954; Martin, 1999). Such tests are expensive and time-consuming. Attempts have also been made to correlate the results from laboratory tests with outdoor exposure data. These methods have, however, often been unsuccessful in predicting coating failures or even in ranking alternative formulations. The lack of timely and accurate predictions have proved to be very costly to both manufacturers and consumers.

Systematic approaches based on mechanistic models of degradation have been proposed to improve the current state of reliability estimation of the materials exposed to the outdoor environment (e.g. Martin, 1999; Meeker, Escobar, and Chan, 2001; Pickett and Gardner, 2001). These approaches involve characterizing the environment stochastically and determining the effects of environmental variables on the degradation or failure mechanisms, both of which are then related through a cumulative damage or degradation model. This model is then used to estimate the reliability or to make service life predictions of the materials in their intended service environment.

This paper proposes a statistical methodology to estimate degradation-based reliability of such materials within the framework of the new approach.

## 1.2 Goal

Quantifying the reliability of materials or products such as paints and coatings involves the prediction of the level of degradation resulting from exposure over time, taking into account the random nature of the outdoor environment. With this in mind, the main

objective of the methodology presented in this paper is to estimate the following:

1. The probability distribution of cumulative degradation at a given point in time.
2. The probability distribution of failure time, or “crossing time”, (i.e., the time at which the cumulative degradation reaches a critical level). The critical level of degradation defines the failure event.

Note that these two distributions arise from the randomness in the environment. They allow us to conduct risk assessment of the failure of the material exposed to outdoor weathering and to characterize its reliability or service life prediction.

### 1.3 Related Work

Most of the literature on methods for reliability analysis focuses on failure time models. There is only a limited amount of literature on degradation-based reliability analysis. Discussion on this subject can be found in Chapter 11 of Nelson (1990), Chapter 7 of Tobias and Trindade (1995), and Chapters 13 and 21 of Meeker and Escobar (1998).

Work on cumulative damage models has been more extensive. Gertsbakh and Kordonsky (1969) present an early work on such models. A survey of the developments of models and pertinent references are given by Saunders (1982). Some relevant work of interest on failure models based on cumulative damage of materials includes Saunders (1970), Bogdanoff and Kozin (1985), and Gillen and Celina (2001).

Bauer and Martin (1999) and Bauer and Martin (2001) describe recent work on the service life prediction associated with paints and coatings exposed to the outdoor environment, including physical and chemical studies of the degradation of such materials. Martin et al. (1996) present and compare the service life prediction methodologies used in the coatings industry with those used in other industries, where such methods have been more successful.

The field of reliability and survival analysis in highly variable environments is currently underdeveloped, with its literatures scattered widely in various different fields. An overview of a large class of failure and cumulative-exposure models based on stochastic processes, with an emphasis on probabilistic modeling, is given by Singpurwalla (1995). This paper also provides key references to work pertaining to the development of such models. Nelson (2001) presents general statistical models and analysis methods using a cumulative damage model to analyze data from accelerated tests with time-varying stresses.

Our work relies on physical/chemical models for failure mechanisms. Such models are described, in the context of accelerated life test models, by Meeker and LuValle (1995),

who present and illustrate a class of accelerated life models based on kinetic failure modes. Reliability models and analysis of data based on accelerated degradation tests are also discussed in Meeker, Escobar and Lu (1998).

## 1.4 Overview

Section 2 describes the model for degradation that forms the foundation of our methodology. Section 3 presents our proposed method to obtain the probability distributions and related reliability metrics of interest by means of time series modeling of predicted daily degradation. The procedure to construct approximate confidence intervals for reliability metrics of interest is discussed in Section 4. In Section 5, an additional example based on a different environment is presented as a further illustration, giving a contrast with the results from the first example.

# 2 Model

## 2.1 Degradation Rate Model

Our approach for evaluating degradation-based reliability requires the use of a physical model that relates degradation rate to relevant environmental factors. The degradation rate function is expressed by  $h(t; \Psi(t), \boldsymbol{\theta})$ , where  $t$  is time,  $\Psi(t)$  is the random vector representing the state of the outdoor environmental variables at time  $t$ , and  $\boldsymbol{\theta}$  is a vector of parameters. The integration of the degradation rate  $h(t; \Psi(t), \boldsymbol{\theta})$  with respect to time will give the cumulative degradation as a function of the length of exposure to the environmental variables, thus capturing the dose-response relationship between the weathering-degradable material and the effects of the environment. Models for degradation rate are obtained by a combination of principles of physical/chemical degradation kinetics and laboratory experiments. If the environmental stress represented by  $\Psi(t)$  is given as a function of time and the parameters in  $\boldsymbol{\theta}$  are known, then the total cumulative degradation or damage is calculated by integrating the degradation rate  $h(t; \Psi(t), \boldsymbol{\theta})$  with respect to time. This is discussed in the next section.

**Example 2.1** Jorgensen et al. (1996) proposed a degradation rate model to describe the degradation of a solar reflector material called ECP-300A. The degradation of the material is measured in terms of change in performance, which is quantified by the material's hemispherical reflectance as a percentage of light reflected. The degradation rate model given

by Jorgensen et al. (1996) depends on three outdoor environmental variables, namely UV radiation, temperature and relative humidity, and has the following form:

$$h(t; \Psi(t), \boldsymbol{\theta}) = \mathcal{A}U(t)T(t)^{-\mathcal{B}}e^{-\mathcal{E}/T(t)}e^{R(t)(\mathcal{C}+\mathcal{D}/T(t))}, \quad (1)$$

where  $U$  is the amount of ultraviolet irradiation in the 290-320nm band (the portion of ultraviolet that reaches the surface of the earth),  $T$  is the temperature on the Kelvin scale and  $R$  is the relative humidity, expressed as a percentage. Here  $\Psi$  corresponds to  $(U, T, R)$  and  $\boldsymbol{\theta}$  to  $(\mathcal{A}, \mathcal{B}, \mathcal{C}, \mathcal{D}, \mathcal{E})$ . Jorgensen et al. (1996) assumed the parameters in  $\boldsymbol{\theta}$  are constant, and conducted an experiment described in detail in their paper to estimate these parameter values. In the laboratory-controlled experiment, different samples of ECP-300A were subjected to various combinations of fixed levels of  $U$ ,  $T$ , and  $R$  for a number of different exposure times. The change in performance (or the cumulative degradation) of each sample was recorded at the end of the experiment. Letting  $\Delta\rho$  denote the change in performance, the statistical model used to fit the data was

$$\Delta\rho = \mathcal{A}I_{UV}T^{-\mathcal{B}}e^{-\mathcal{E}/T}e^{R(\mathcal{C}+\mathcal{D}/T)} + \epsilon,$$

where  $I_{UV}$  is the cumulative UV dose over exposure time, and  $\epsilon$  represents the error term. The value of  $\boldsymbol{\theta} = (\mathcal{A}, \mathcal{B}, \mathcal{C}, \mathcal{D}, \mathcal{E})$  was estimated using nonlinear least squares. The estimates are:  $\hat{\mathcal{A}} = 3.5 \times 10^5 \text{ K}^{\mathcal{B}}\text{m}^2/\text{J}$ ,  $\hat{\mathcal{B}} = -1.22$ ,  $\hat{\mathcal{C}} = 0.132$ ,  $\hat{\mathcal{D}} = -40.1\text{K}$ ,  $\hat{\mathcal{E}} = 2339\text{K}$ . Under the assumption that  $\epsilon$  follows a normal distribution, the estimates are equivalent to maximum likelihood (ML) estimates.

The model in (1) is known as an Eyring model (Eyring, Gladstones, and Laidler, 1941). In most applications of this model, the parameter  $\mathcal{B}$  is assumed to be given and typical values are in the range of 0 to 1. This parameter is supposed to be related to the nature of the chemical reaction, but is rarely known in practice and is difficult to estimate from data because its estimates will be highly correlated with  $\mathcal{E}$  and  $\mathcal{D}$ . In this paper we will set  $\mathcal{B} = 0$ . This special case of the Eyring model corresponds to the commonly used Arrhenius model for rate dependence on temperature. Using the Arrhenius model reduces the number of parameters of the model from five to four. Because the terms inside the exponential dominate in determining the rate, this modification has only a small effect on the output of the model.

The least squares estimates of the parameters of this reduced model are  $\hat{\mathcal{A}} = 0.1023 \text{ m}^2/\text{J}$ ,  $\hat{\mathcal{C}} = 0.1299$ ,  $\hat{\mathcal{D}} = -40.08\text{K}$ ,  $\hat{\mathcal{E}} = 2634.9 \text{ K}$ . Comparisons between the degradation patterns from the simplified model and from Jorgensen et al.'s model resulting from the outdoor environments show very little difference.

□

## 2.2 General Model

Given the degradation rate model  $h(t; \Psi(t), \boldsymbol{\theta})$ , the total cumulative degradation at time  $t$  is

$$D(t; \Psi[0, t], \boldsymbol{\theta}) = D_0 + \int_0^t h(\tau; \Psi(\tau), \boldsymbol{\theta}) d\tau \quad (2)$$

where  $\Psi[0, t]$  denotes the stochastic process representing the environmental factors in the time interval  $[0, t]$ , and  $D_0$  is the level of degradation at time 0. In physical/chemical applications, the degradation rate  $h(t; \Psi(t), \boldsymbol{\theta})$  is typically a nonnegative function, so that the cumulative degradation  $D(t; \Psi[0, t], \boldsymbol{\theta})$  is nondecreasing. Throughout this paper, we assume that the parameter vector  $\boldsymbol{\theta}$  is fixed but unknown.

If the value of the parameter vector  $\boldsymbol{\theta}$  were known, along with the values of the environmental variables in  $\Psi(t)$  at a sufficiently small resolution over the time interval of interest, it would be straightforward to compute the total cumulative degradation by integrating the degradation rate  $h(t; \Psi(t), \boldsymbol{\theta})$  over time. A simple quadrature formula such as the trapezoidal rule could then be used to evaluate the integral and thus obtain the cumulative degradation. Therefore, if a stochastic model for the  $\Psi(t)$  were available, we could evaluate the probability distributions of cumulative degradation and failure time by employing Monte Carlo simulation.

## 2.3 Reliability Metrics of Interest

The failure level  $a$  is defined as the level of degradation above which the degradation is said to have reached failure, i.e., the failure event is  $\{D(t; \Psi[0, t], \boldsymbol{\theta}) \geq a\}$ . For a specified failure level  $a$ , reliability metrics of interest are

1. The probability of failure at a given time  $t$ , i.e.,  $\Pr(D(t; \Psi[0, t], \boldsymbol{\theta}) \geq a)$ .
2. The  $p$  quantile,  $t_p$ , of the failure time distribution, where the failure time  $T_f$  is defined as the time the cumulative degradation first crosses the failure level  $a$ , i.e.,  $T_f = \inf(t : D(t; \Psi[0, t], \boldsymbol{\theta}) \geq a)$ .

As an illustration of the two metrics, consider a material that degrades exponentially when exposed to the outdoor elements. Figure 1 shows ten degradation paths (degradation as a function of time) for continuous weathering up to  $t = 5$  time units. Each degradation path represents an environmental realization of  $\Psi[0, 5]$ . The bell-shaped distribution at the end of the paths represents the distribution of the cumulative degradation of the material at  $t = 5$ . The fraction of the distribution that exceeds the failure level  $a = 30$  is the probability of failure  $\Pr(D(t; \Psi[0, t], \boldsymbol{\theta}) \geq a)$ . In Figure 2, the distribution at the top of

the ten degradation paths corresponds to the distribution of failure time  $T_f$ . Then  $t_p$  is the  $p$  quantile of the distribution.

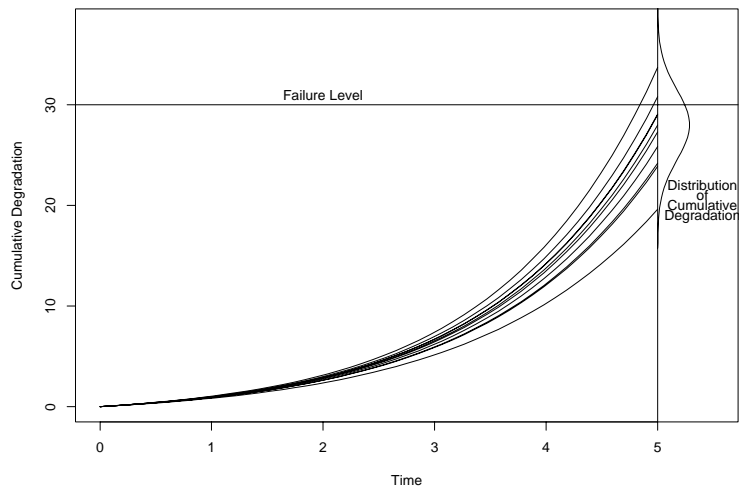


Figure 1: Ten Degradation Paths with Exponential Degradation, and Cumulative Degradation distribution at  $t = 5$ .

Note that because of the nondecreasing nature of the degradation path, there exists a direct relationship between the two metrics. The failure time  $T_f$  and the probability of failure at time  $t$  are related by

$$\Pr(T_f \leq t) = \Pr(D(t; \Psi[0, t], \boldsymbol{\theta}) \geq a).$$

There also exists an equivalent relationship for failure time quantiles. Let  $p$  be the probability of failure at time  $t = t'$  for some specified failure level. Then for the same failure level, the  $p$  failure time quantile  $t_p$  is equal to  $t'$ , i.e.,  $t_p = t'$ .

## 2.4 Weather Data

Weather data are used to characterize the stochastic outdoor environment. Such data are available from a number of public and private sources. The weather data that we will use in conjunction with the degradation model for solar reflector materials were obtained from the SURFRAD network, a program established by National Oceanic and Atmospheric

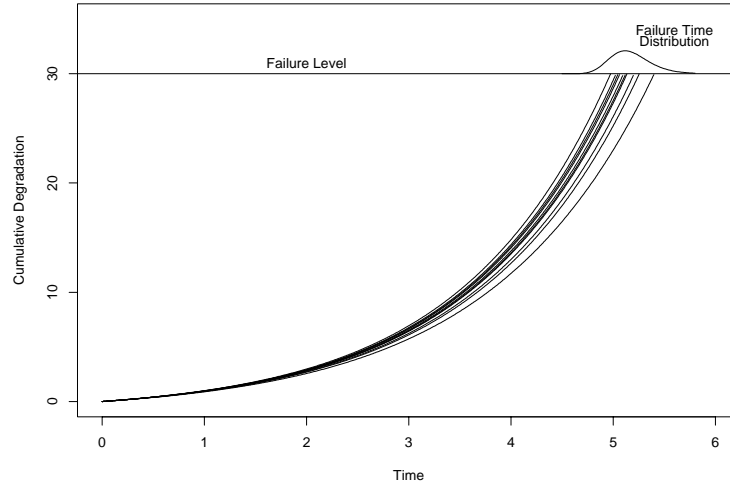


Figure 2: Ten Degradation Paths with Exponential Degradation, and Failure Time Distribution, with Failure Level at  $a = 40$ .

Administration (NOAA) in 1993. This network of stations monitors and collects measurements on surface radiation in the United States. The data from SURFRAD consist of observations on radiation variables such as global solar ultraviolet radiation in the UV-B band (290-320 nm) and infrared radiation. SURFRAD also provides data on other meteorological parameters such as temperature, relative humidity, windspeed, and atmospheric pressure. Observations are made every 3 minutes every day of the year. The six monitoring stations in the network are located in Montana, Colorado, Illinois, Mississippi, Pennsylvania and Nevada. Weather data and information on SURFRAD are available at [www.srrb.noaa.gov/surfrad/surfpag.htm](http://www.srrb.noaa.gov/surfrad/surfpag.htm). Some of the data sets contain missing observations due mostly to breakdown in measuring instruments. The amount of missing data, however, is typically small, on the order of a few percent of the total data. In our proposed methodology, the missing values within the weather data are handled as described in Section 3.1.

We will use the data from the station at Boulder, Colorado to demonstrate our methodology. In Section 5 we will provide a second contrasting example based on the data from Fort Peck, Montana.

## 2.5 Issues on the Modeling of the Environment

Analytical methods to obtain probability distributions of interest within the framework of the model given in (2) generally do not exist for practical problems involving complicated and highly variable environments such as the outdoor weather. With modern computing capabilities, however, simulation-based methods provide another way to evaluate the distributions. Given a model for the degradation rate and a stochastic model for the environmental variables, we could evaluate the distributions by the following steps:

1. Use the environmental model to generate a large number of realizations that simulate the environmental outcomes.
2. For each realization, use a quadrature rule to approximate the integral in (2). This yields cumulative degradation as a function of time, or the degradation path.
3. A large collection of such degradation paths can be used to obtain the probability distributions such as those described in Section 1.2.

An adequate parametric stochastic model for the outdoor environment may not, however, be readily available. The statistical modeling of the environmental variables by means of a multivariate time series model (which is necessary for Monte Carlo simulation) is difficult due to a combination of the following reasons:

- Weather variables such as solar radiation and temperature have complicated and highly variable behaviors, especially at a small temporal scale. The intensities of these variables are influenced by ever-changing meteorological components such as cloud cover and large-scale air movement.
- Relative humidity has an upper bound at 100%, which is frequently realized (for example, during rain or snow events). This requires modeling a distribution with a discrete component.
- There are both within-year (or seasonal) and within-day (hour-to-hour or minute-to-minute) periodicity and variability to describe.
- In addition to autocorrelation of each environmental variable, the multivariate time series model must capture the cross correlation among the variables (which may be three or more in number). The correlations may vary with time of day or time of year.
- Most of the available theory for handling multivariate time series and other problems with correlated data use an underlying Gaussian error structure. The outdoor en-

environmental variables at small temporal scales have non-Gaussian behaviors, and so cannot be modeled by such an error structure.

The following section describes an alternative approach that avoids the need for an explicit parametric joint stochastic model for the outdoor environmental variables.

### 3 Time Series Modeling of Predicted Daily Degradation

This section describes the time series modeling of predicted daily degradation to obtain degradation-related distributions. The first subsection briefly describes the scheme, followed by an example of the implementation of this scheme using the degradation model for the solar reflector material and the data from Boulder, Colorado.

#### 3.1 Predicted Daily Degradation

The basic idea of our procedure is to characterize the predicted incremental degradation accumulated within each 24-hour day using a time series model and use the model for simulation. This has the advantage of having to deal with only a univariate time series, as opposed to the more complicated multivariate data when modeling the entire set of environmental variables responsible for the degradation.

The daily degradation accumulated in day  $i$  is defined as

$$W_i = \int_{\text{day } i} h(t; \Psi(t), \boldsymbol{\theta}) dt. \quad (3)$$

The total cumulative degradation for  $t = n$  days are then related to the daily degradation  $W_i$  by

$$\begin{aligned} D(t; \Psi[0, t], \boldsymbol{\theta}) &= \int^t h(t; \Psi(t), \boldsymbol{\theta}) dt \\ &= \sum_{i=1}^n \int_{\text{day } i} h(t; \Psi(t), \boldsymbol{\theta}) dt = \sum_{i=1}^n W_i, \end{aligned} \quad (4)$$

where for simplicity, we have let  $D_0 = 0$ .

Computing the daily degradation  $W_i$  using past weather data for  $\Psi(t)$  yields predicted daily degradation (PDD) data, a quantity not directly observed but estimated by the degradation rate model. The PDD data are much easier to model than the environmental factors in  $\Psi(t)$ , not only because the PDD data are univariate, but also because they have

a much larger temporal scale (daily scale) than  $\Psi(t)$ .  $\Psi(t)$  requires a small resolution so that numerical approximations can be used in the algorithm described in Section 2.5.

Having computed the PDD for each day in our weather data, the next step is to describe the  $W_i$  sequence by means of a univariate time series model. Then this model is used to simulate future values of  $W_i$ . Summing the sequence of simulated  $W_i$  values yields a simulated realization of  $D(t; \Psi[0, t], \theta)$ .

**Example 3.1** Figure 3 shows a plot of the PDD values for solar reflector materials exposed to the outdoor elements over a period of about five years in Boulder, Colorado. Each PDD value was computed by numerically integrating the degradation rate model given in(1) for a one-day period using radiation, temperature and relative humidity from the SURFRAD data at three-minute resolution from November 1995 to August 2000. Missing PDD values resulting from missing observations in the weather dataset (which are on the order of a few percent) were substituted by the mean PDD values of their corresponding day of the year. We obtained these mean PDD values by smoothing the empirical daily mean values, a procedure described in Section 3.2 (i.e.,  $b_i$  values in that section).

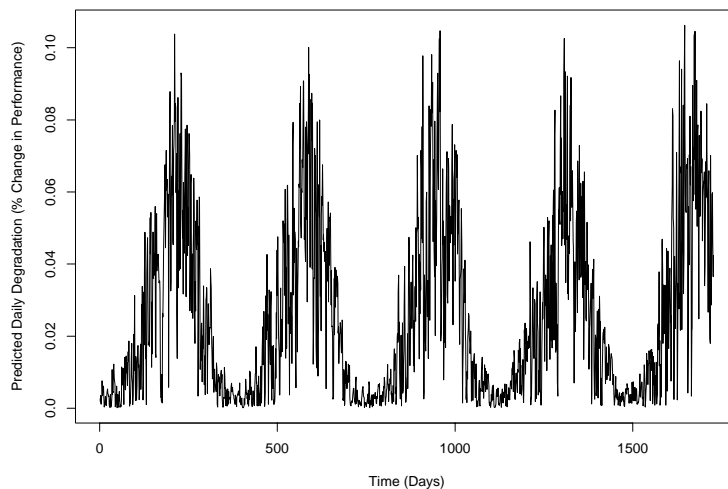


Figure 3: Predicted Daily Degradation  $W_i$  in Boulder, CO from Nov. 1995 to Aug. 2000.

The plot shows a strong seasonal trend and day-to-day variability. The variation from day to day is more pronounced during the warm months. The time-series indicates the

possibility of modeling the daily degradation  $W_i$  as a stationary time series after removing the seasonal pattern and adjusting for the seasonal-dependent variance.  $\square$

### 3.2 Seasonal Adjustment of Predicted Daily Degradation

Typically the degradation rate  $h(t; \Psi(t), \theta)$  is an increasing function of the environmental variables contained in  $\Psi(t)$ . For example, the higher the temperature or the more intense the radiation, the faster the degradation process (this is the case with the solar reflector degradation model). Because  $W_i$  is obtained by integrating  $h(t; \Psi(t), \theta)$  with respect to time over day  $i$ ,  $W_i$  for a particular day with larger values of  $\Psi(t)$  will be greater than that for one with smaller values of  $\Psi(t)$ . The outdoor environmental variables such as temperature and ultraviolet radiation are highly seasonal. Therefore, PDD will typically exhibit the same seasonal pattern as the daily temperature and solar radiation, with on the average a peak in the summer and a valley during winter months. This behavior is seen in the PDD data for the solar reflector materials given in Example 3.1.

As such, modeling PDD consists of extracting the seasonal component of the data and adjusting for the daily variation, and then modeling the residuals. This is a commonly used modeling procedure for time series data. The residuals are here referred to as “standardized” daily degradation  $X_i$  and are obtained from

$$X_i = \frac{W_i - b_i}{a_i}, \quad (5)$$

where here  $W_i$  represents PDD,  $b_i$  accounts for the seasonal mean, and  $a_i$  is a scale factor to adjust possible day-to-day variability. Ignoring the extra day in leap years for simplicity, both  $a_i$  and  $b_i$  have a period of 365 days. Their values depend on the day of the year corresponding to index  $i$ .

To obtain the values for  $a_i$  and  $b_i$ ,  $i = 1, 2, \dots, 365$ , we first compute the mean and the standard deviation for PDD data corresponding to each day of the year, the so-called Julian day. Then the daily means and daily standard deviations are smoothed to yield  $b_i$  and  $a_i$ . Smoothing is needed because physical considerations suggest that  $a_i$  and  $b_i$  be “smooth” functions of Julian day  $i$ ; the daily means and standard deviations computed from limited amount of data such as ours typically lack the necessary smoothness. Possible local smoothing methods include spline and kernel smoothers, which are available in many statistical softwares. For the work in this paper, however, we used a Fourier series model because the periodic nature of meteorological or weather-induced variables can be described parsimoniously in terms of sines and cosines.

**Example 3.2** The plots of mean and standard deviation, along with their smoothed values, of PDD corresponding to Boulder, Colorado for each Julian day are given in Figures 4 and 5. We used a Fourier series with two low-order harmonic terms to smooth the  $a_i$  and  $b_i$  values.

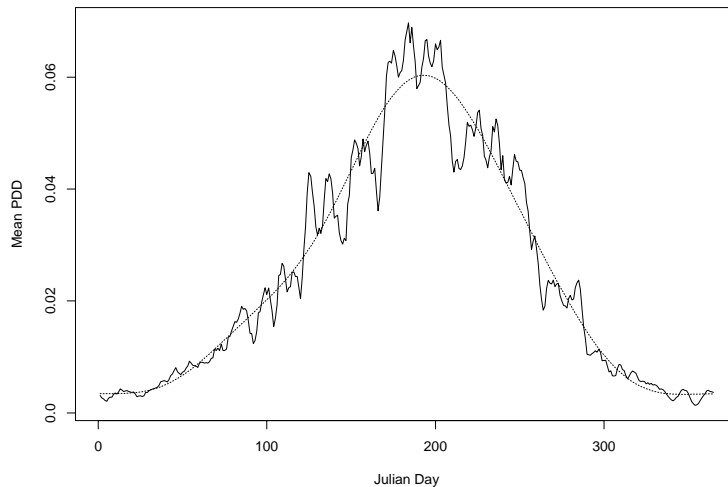


Figure 4: Plot of Average PDD in Boulder, CO for each Day of the Year, and the fitted Fourier Series model.

The standardized PDD  $X_i$  for Boulder, Colorado, computed using the expression in (5), is given in Figure 6. The plot suggests that the  $X_i$  process is stationary, and can perhaps be appropriately modeled by an autoregressive (AR) model.

□

### 3.3 Modeling Predicted Daily Degradation and Simulation

For given  $a_i, b_i$ ,  $i = 1, \dots, 365$ , modeling  $X_i$  is equivalent to modeling  $W_i$ . For the data that we have investigated, AR models appear to be appropriate.

Having found the time series model for the standardized PDD, daily degradation  $X_i$ , and hence  $W_i$ , we can obtain the distribution of degradation at a future time or the distribution of failure time through Monte Carlo simulation. To simulate a degradation path, we first generate a sequence of  $X_i$  values using the AR model, either by resampling the AR model residuals for  $\epsilon_i$ , or by fitting a distribution to the residuals (which should be

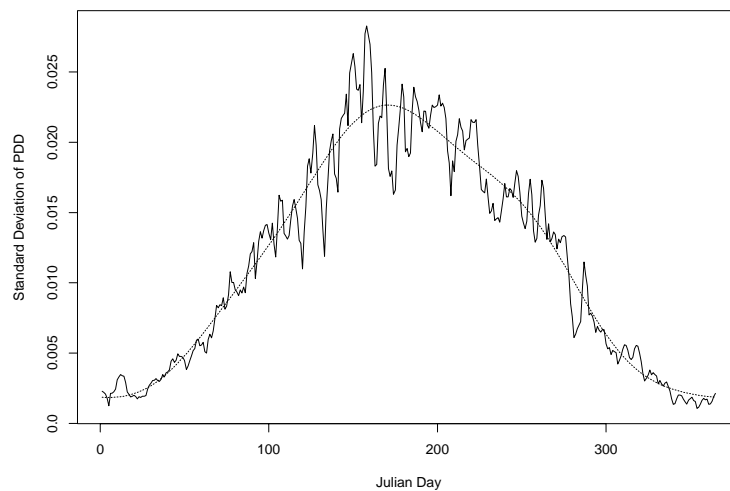


Figure 5: Plot of the Standard Deviation of PDD in Boulder, CO for each Day of the Year, and the fitted Fourier Series model.

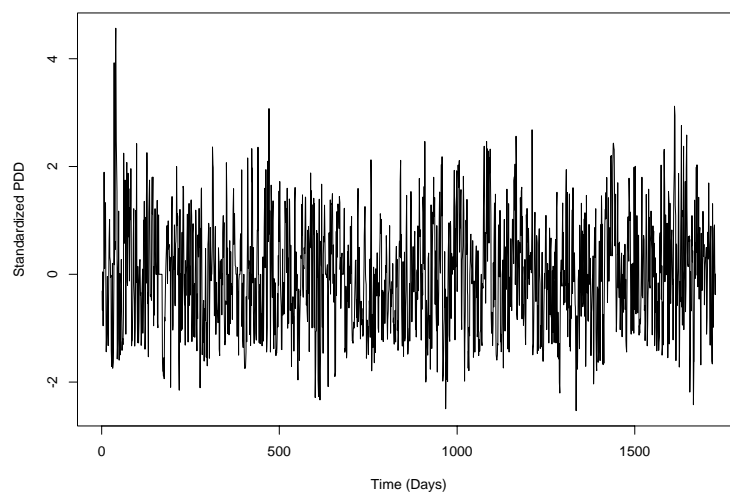


Figure 6: Plot of Standardized PDD  $X_i$  for Boulder, CO from Nov. 1995 to Aug. 2000.

approximately iid) and drawing random samples from this distribution. In large samples, these two methods for generating  $\epsilon_i$  yield similar results. The first method, however, is preferred when a large data set is available because it does not require modeling and is therefore easier to carry out. Having obtained a sequence of  $X_i$  values, we then transform each value of  $X_i$  back to  $W_i$  by multiplying by the corresponding factor  $a_i$  and relocating by adding the appropriate  $b_i$ , and finally we sum them up. The simulated degradation paths can then be used to estimate the probability distributions of interest.

**Example 3.3** For the standardized PDD  $X_i$  shown in Figure 6 corresponding to Boulder, Colorado, a time series analysis using the autocorrelation function (ACF) and the partial autocorrelation function (PACF) plots suggest that a low-order AR model may be appropriate. Using ML estimation with AIC criterion (see, for example, Brockwell and Davis (1995), p. 169 ) suggested an AR(1) model

$$X_i = \phi_1 X_{i-1} + \epsilon_i$$

with parameters  $\hat{\phi}_1 = 0.49$  is selected. Model diagnostics indicate that the AR(1) model is adequate. Fitting an AR(2) or AR(3) model to the data instead and comparing the results with those for AR(1) suggests that the final results (e.g. distributions related to cumulative degradation) are robust with respect to the choice of the order of the AR model.

Figure 7 shows a plot of ten simulated degradation paths through a period of five years in Boulder, Colorado, starting on January 1 and assuming the initial degradation  $D_0 = 0$ . The sinusoidal shape of the paths is due to seasonal change. The steep slopes in each path correspond to summer months, when the degradation rate is highest due to the longer days, higher temperature, and more intense solar radiation. During winter the environmental conditions are less harmful to the degradable material, and so the degradation rate is slow by comparison, demonstrated by the nearly zero slopes.

□

### 3.4 Estimation of the Distributions of Cumulative Degradation

The distribution of total cumulative degradation at any given point in time can be approximated by simulating a large number of the degradation paths and using the empirical distribution of the cumulative degradation at the given time point.

The limiting distribution of the cumulative degradation when the time of prediction becomes very large provides a useful approximation. With an AR( $p$ ) model for  $X_i$ , the

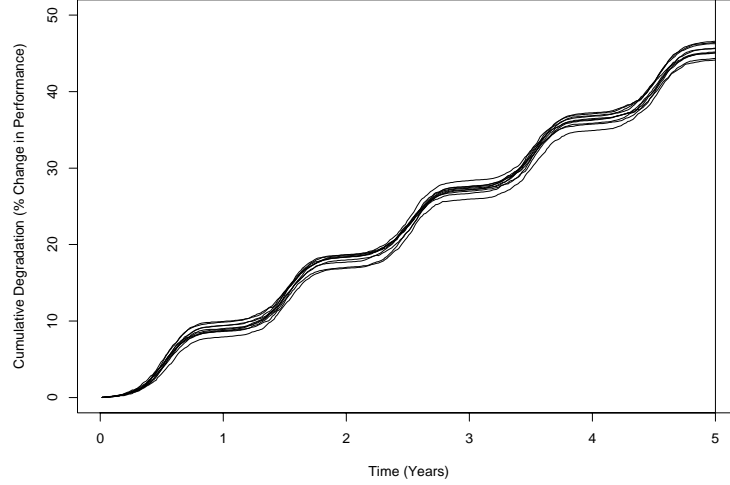


Figure 7: Ten Simulated Degradation Paths from Time Series Modeling of Daily Degradation for Boulder, CO, starting on January 1 and assuming  $D_0 = 0$ .

distribution of  $\sum_{i=1}^n a_i X_i$  tends to normal as  $n$  increases (by using Theorem 6.3.4, p. 329, Fuller (1996)), and therefore the cumulative degradation  $\sum_{i=1}^n a_i W_i$  tends to normal also. To be more precise, the distribution of the total cumulative degradation with an AR( $p$ ) model for  $t = r$  years when  $r$  is large, is

$$D(t; \Psi[0, t], \boldsymbol{\theta}) \sim N\left(D_0 + r \sum_{i=1}^{365} b_i, r \left(\sum_{i=1}^{365} a_i^2\right) V\right), \quad (6)$$

where  $V$  depends on the order of the AR( $p$ ) model and its parameter values. The derivation of this result is given in Appendix A.

**Example 3.4** Figure 8 represents the distribution of the total cumulative degradation in Boulder, CO in five years of exposure, based on using 10,000 simulated degradation paths.

The bell-shaped curve of the histogram suggests a normal distribution for the cumulative degradation. The normal probability plot of the histogram in Figure 8 substantiates the normal distribution behavior of the cumulative degradation. This result is consistent with the limiting result in (6). For solar reflector materials exposed to the outdoor elements in Boulder and using AR(1) model,  $\sum_{i=1}^{365} b_i = 9.054$  and  $(\sum_{i=1}^{365} a_i^2) V = 0.20727$ . For five years, the mean and standard deviation of the total cumulative degradation according

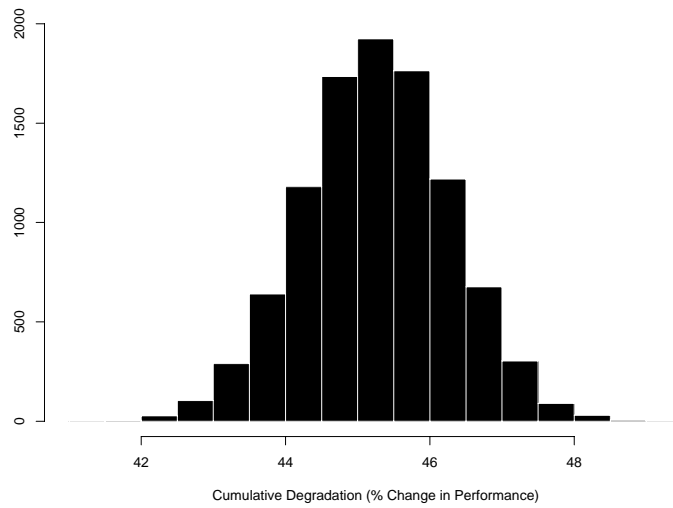


Figure 8: Histogram of Total Cumulative Degradation in 5 Years using 10,000 Simulated Degradation Paths for Boulder, CO.

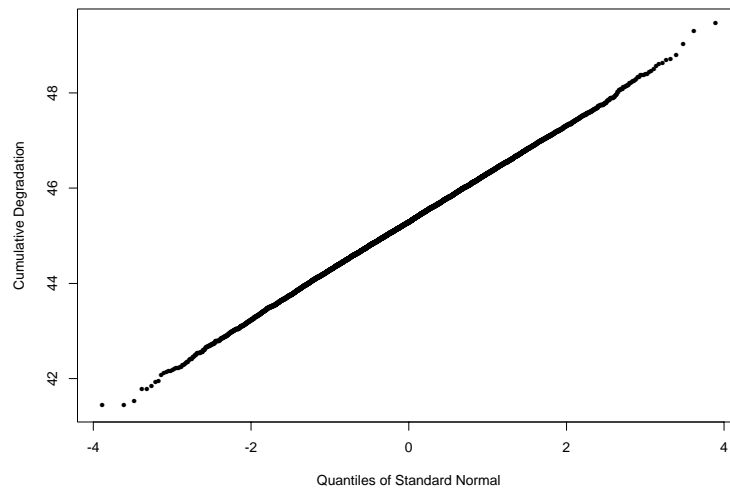


Figure 9: Normal Probability Plot of Total Cumulative Degradation in 5 Years using 10,000 Simulated Degradation Paths for Boulder, CO.

to (6) are  $9.054 \times 5 = 45.27$  and  $\sqrt{0.20727 \times 5} = 1.018$ . As a comparison, the mean and standard deviation of the distribution of simulated cumulative degradation depicted in the histogram are 45.26 and 1.017, respectively.

□

### 3.5 Estimation of the Distribution of Failure Time

As in the case of the distribution of cumulative degradation, simulated degradation paths can be used to estimate the distribution of failure time. To do this, we first generate a degradation path  $D(t)$  and note the time when it hits the failure level  $a$ . Repeating the procedure a large number of times will give an estimate of the failure time distribution. Based on this distribution, reliability metrics of interest such as failure time quantiles and failure probabilities can be estimated.

**Example 3.5** Figure 10 shows ten simulated degradation paths for the solar reflector material exposed to the weather conditions at Boulder under the specification that the failure level is at 50% loss in reflectance and assuming  $D_0 = 0$ . The histogram in Figure 11 gives the corresponding distribution of failure time using 10,000 simulations at the failure level of 50%.

□

## 4 Approximate Confidence Interval for Reliability Metrics

The method described in Section 3 allows for the evaluation of the distributions of cumulative degradation and failure time resulting from the variability in the environment for a given model parameter vector  $\theta$ .  $\theta$  is assumed to be fixed but unknown, and their estimated values are used throughout the implementation of the procedure.

There is, however, uncertainty associated with  $\theta$ . Confidence intervals for the reliability metrics related to the degradation, such as the probability of failure in  $r$  years and the failure quantile for a given failure level, can be used to reflect this uncertainty.

### 4.1 Reliability Metrics as a Function of $\theta$

One straightforward way to obtain the confidence intervals is by using the large-sample normal approximation method for maximum likelihood (ML) estimate. In what follows, we

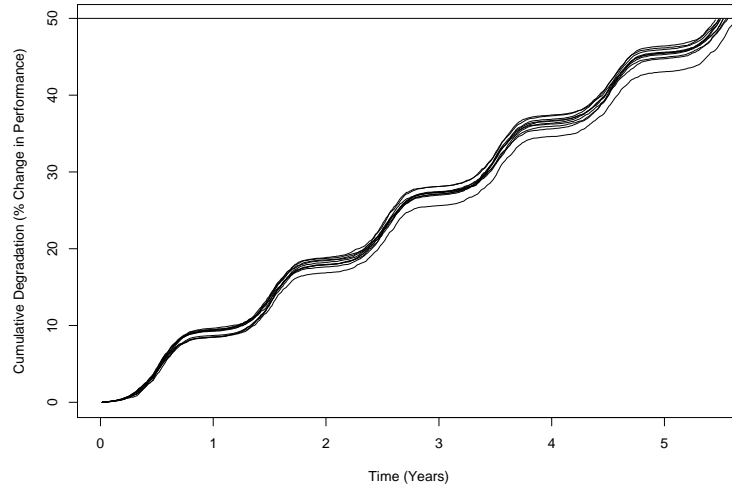


Figure 10: Ten Simulated Degradation Paths from Daily Degradation Modeling of Boulder, CO Weather Data, with a Failure Level at 50%, starting on January 1 and assuming  $D_0 = 0$ .

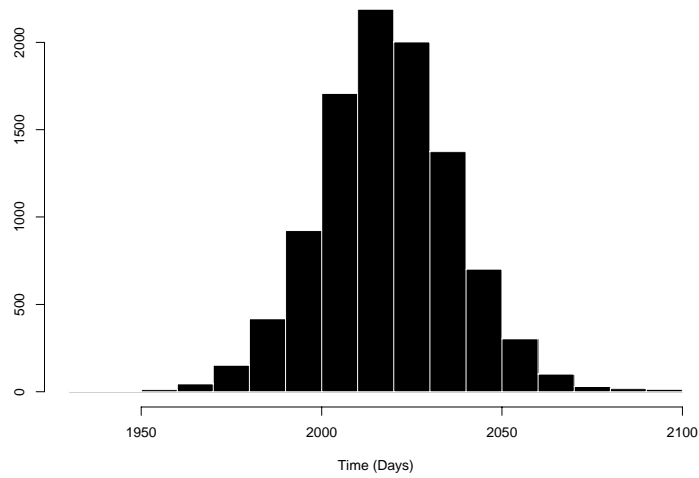


Figure 11: Histogram of Failure Times for Boulder, CO with a Failure Level at 50%, based on 10,000 Simulated Degradation Paths.

will illustrate the computation of confidence intervals only for  $t_p$ , the  $p$  failure time quantile at some specified level of failure. Application of the method for other functions of  $\boldsymbol{\theta}$  such as the probability of failure in  $r$  years is similar. For simplicity, we will suppress the notation of degradation rate model and weather in the following discussion. This is because, even though they do affect  $t_p$ , the degradation rate model and the complete weather data set for the given location are fixed inputs.

Under our time series modeling scheme, the failure time quantile is a function of  $\boldsymbol{\theta}$  and a time series model for the daily degradation that also depends on  $\boldsymbol{\theta}$ , i.e.,

$$t_p = g(\boldsymbol{\theta}, TSM\{\boldsymbol{\theta}\}).$$

Here  $TSM\{\boldsymbol{\theta}\}$  denotes a time series model among the set of models that adequately describe the daily degradation  $W_i$  generated by using  $\boldsymbol{\theta}$  in the degradation rate model.  $TSM\{\boldsymbol{\theta}\}$  appears as an argument of the function is because there are more than one competing time series model for modeling the daily degradation  $W_i$  and each adequate model is likely to yield a different value of  $t_p$ .

For constructing confidence intervals, we will use numerical perturbation of  $\boldsymbol{\theta}$  about  $\hat{\boldsymbol{\theta}}$ . Small perturbations of  $\boldsymbol{\theta}$  about  $\hat{\boldsymbol{\theta}}$  typically do not affect the parametric model used to describe the data generated by  $\hat{\boldsymbol{\theta}}$ . This is true of our example involving the daily degradation  $W_i$  for Boulder, for which the AR model of the same order is enough to describe the standardized  $W_i$ 's corresponding to small perturbations about  $\hat{\boldsymbol{\theta}}$ . As such, it is enough to fix the time series model. Then the failure time quantile is a function of just  $\boldsymbol{\theta}$ , i.e.,  $t_p = g(\boldsymbol{\theta})$ .

The standard construction of normal-approximation confidence interval with ML estimators can now be applied. This will be discussed briefly in the next section.

## 4.2 Procedure for Constructing Approximate Confidence Intervals

Suppose that  $t_p = g(\boldsymbol{\theta})$ . Let  $\hat{\boldsymbol{\theta}}$  denote the ML estimate of  $\boldsymbol{\theta}$ . Then by the invariance property of ML estimators,  $\hat{t}_p = g(\hat{\boldsymbol{\theta}})$ . The covariance matrix of  $\hat{\boldsymbol{\theta}}$ ,  $\hat{\Sigma}_{\hat{\boldsymbol{\theta}}}$ , is typically computed in ML estimation, and an estimate of the variance of  $\hat{t}_p$  is given by

$$\widehat{\text{Var}}(\hat{t}_p) = \left[ \frac{\partial g(\boldsymbol{\theta})}{\partial \boldsymbol{\theta}} \right]' \hat{\Sigma}_{\hat{\boldsymbol{\theta}}} \left[ \frac{\partial g(\boldsymbol{\theta})}{\partial \boldsymbol{\theta}} \right],$$

where the derivatives are evaluated at  $\boldsymbol{\theta} = \hat{\boldsymbol{\theta}}$ . The expression for the variance requires the computation of the partial derivative of each parameter in the parameter vector  $\boldsymbol{\theta}$ . Because

no closed-form expressions are available for these derivatives in our estimation procedure, the estimation of the variance is accomplished by using numerical perturbation.

Under suitable regularity conditions, the limiting distribution of studentized  $\hat{t}_p = g(\hat{\boldsymbol{\theta}})$  is normal, i.e.,

$$\frac{\hat{t}_p - t_p}{\sqrt{\widehat{\text{Var}}(\hat{t}_p)}} \sim N(0, 1),$$

so that an approximate  $100(1 - \alpha)\%$  normal-approximation confidence interval is given by

$$\hat{t}_p \pm z_{(1-\alpha/2)} \sqrt{\widehat{\text{Var}}(\hat{t}_p)},$$

where  $z_{1-\alpha/2}$  is the  $1 - \alpha/2$  quantile of the standard normal distribution.

An alternative method for constructing a confidence interval for a positive quantity is to use the approximation

$$\frac{\log(\hat{t}_p) - \log(t_p)}{\sqrt{\widehat{\text{Var}}(\log(\hat{t}_p))}} \sim N(0, 1),$$

where  $\sqrt{\widehat{\text{Var}}(\log(\hat{t}_p))} = \sqrt{\widehat{\text{Var}}(\hat{t}_p)/\hat{t}_p}$ . For more discussion on the use of this assumption, see Meeker and Escobar (1998, p. 163). Then an approximate  $100(1 - \alpha)\%$  confidence interval is given by

$$[\hat{t}_p/w, \hat{t}_p w], \tag{7}$$

where  $w = \exp \left[ z_{(1-\alpha/2)} \sqrt{\widehat{\text{Var}}(\hat{t}_p)/\hat{t}_p} \right]$ . This approach has the advantage that the interval endpoints are always positive. We will use this approach for construction of a confidence interval in the following example.

**Example 4.1** The ML estimate of  $\boldsymbol{\theta}$  is given in Example 2.1. The covariance matrix for  $\hat{\boldsymbol{\theta}} = (\log \hat{\mathcal{A}}, \hat{\mathcal{C}}, \hat{\mathcal{D}}, \hat{\mathcal{E}})$  is

$$\hat{\Sigma}_{\hat{\boldsymbol{\theta}}} = \begin{bmatrix} 3.3988 & -0.045322 & 14.589 & -1094.2 \\ -0.045322 & 0.0016402 & -0.53596 & 14.589 \\ 14.589 & -0.53596 & 176.01 & -4728.5 \\ -1094.2 & 14.589 & -4728.5 & 354649.0 \end{bmatrix}.$$

We shall consider  $t_{.25}$ , the .25 quantile of the failure-time distribution, for Boulder. To compute the variance of  $\hat{t}_{.25}$ ,  $\partial g(\boldsymbol{\theta})/\partial \boldsymbol{\theta}$ , the partial derivative of  $g(\boldsymbol{\theta})$  with respect to each parameter, will have to be calculated. The four plots in Figure 12 show the change in  $\hat{t}_{.25}$  versus a small change in parameters  $\mathcal{A}$ ,  $\mathcal{C}$ ,  $\mathcal{D}$  and  $\mathcal{E}$ . Each value of  $\hat{t}_{.25}$  in the plot was

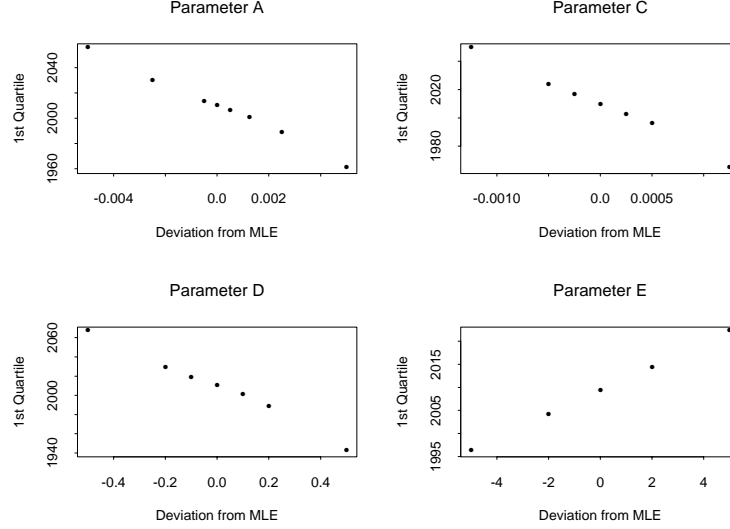


Figure 12: Plots of Change in  $\hat{t}_{.25}$  versus Change in each of the 4 Parameters for Boulder, CO.

obtained from 10,000 simulations. The linear trend in each plot suggests that the slope can be used to approximate the partial derivative. Therefore we have

$$\begin{aligned}
 \left. \frac{\partial g(\boldsymbol{\theta})}{\partial \boldsymbol{\theta}} \right|_{\hat{\boldsymbol{\theta}}} &= \left( \frac{\partial g(\boldsymbol{\theta})}{\partial \log \mathcal{A}}, \frac{\partial g(\boldsymbol{\theta})}{\partial \mathcal{C}}, \frac{\partial g(\boldsymbol{\theta})}{\partial \mathcal{D}}, \frac{\partial g(\boldsymbol{\theta})}{\partial \mathcal{E}} \right) \Big|_{\hat{\boldsymbol{\theta}}} \\
 &= \left( \mathcal{A} \frac{\partial g(\boldsymbol{\theta})}{\partial \mathcal{A}}, \frac{\partial g(\boldsymbol{\theta})}{\partial \mathcal{C}}, \frac{\partial g(\boldsymbol{\theta})}{\partial \mathcal{D}}, \frac{\partial g(\boldsymbol{\theta})}{\partial \mathcal{E}} \right) \Big|_{\hat{\boldsymbol{\theta}}} \\
 &= (-711.32, -28000, -100, 2.586)
 \end{aligned}$$

and so

$$\text{Var}(\hat{t}_{.25}) = \left[ \frac{\partial g(\boldsymbol{\theta})}{\partial \boldsymbol{\theta}} \right]' \hat{\Sigma}_{\hat{\boldsymbol{\theta}}} \left[ \frac{\partial g(\boldsymbol{\theta})}{\partial \boldsymbol{\theta}} \right] = 8765217.$$

The value of  $\hat{t}_{.25}$  obtained from simulation is equal to 2009 days, or about five and a half years. Since  $w = \exp(z_{0.95} \sqrt{\widehat{\text{Var}}(\hat{t}_p)/\hat{t}_p}) = \exp(1.96 \sqrt{8765217}/2009) = 17.96$ , by the expression in (7) an approximate 95% confidence interval for  $t_{.25}$  is

$$[2009/17.96, \quad 2009 \times 17.96] = [112, \quad 36081].$$

The interval is extremely wide. This is the result of the large uncertainty in the parameters  $\mathcal{A}$ ,  $\mathcal{C}$ ,  $\mathcal{D}$  and  $\mathcal{E}$ , reflected in the covariance matrix. The interval width could be reduced by using a larger sample size in the laboratory test and by designing a test to

focus on particular reliability metrics of interest. Use of repeated measures of degradation on each solar reflector material sample instead of the single measure reported by Jorgensen et al. (1996) would also have improved estimation precision.

□

## 5 Additional Example: Fort Peck, Montana

As further application of the methodology of modeling the daily degradation and comparison to the results from the Boulder data, we will present the results for using the degradation rate model for solar reflector materials and the weather data from Fort Peck, Montana in this section.

The PDD data for Fort Peck, Montana is shown in Figure 13. Comparing them with Figure 3, we see that the Boulder PDD data have higher peaks and larger variability than the Fort Peck data. Fort Peck lies at a higher latitude than Boulder ( $48.3^\circ$  North vs.  $40.1^\circ$  North), and therefore the average daily amount of solar radiation it receives is less and the average temperature is lower than those in Boulder. This explains its lower average peak. Also for the same reason, there is less degradation during winter months with less variability.

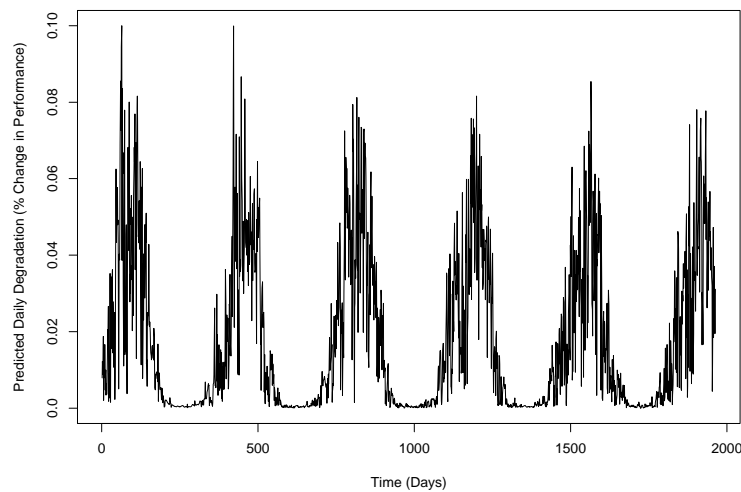


Figure 13: Estimated Daily Degradation  $W_i$  in Fort Peck, MT from Apr. 1995 to Aug. 2000.

As for the modeling of the Fort Peck standardized daily degradation  $X_i$ , the ACF and PACF plots indicate that an AR(5) or an AR(8) process might be a good model. Fitting an AR model with an AIC criterion gives an AR(5) model with parameters  $\Phi = (0.494, -0.0246, 0.0524, -0.00441, 0.0678)$ . Using this AR model gives us the histogram of total cumulative degradation in five years shown in Figure 14. Compared with the histogram for Boulder in Figure 8, the mean total cumulative degradation for Fort Peck is much smaller than that for Boulder (30.08 vs. 45.26), as expected. The variance for Fort Peck is also smaller (0.824 vs. 1.035).

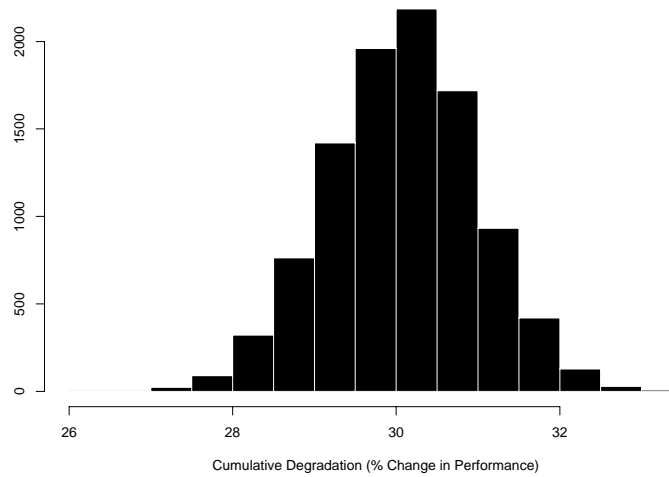


Figure 14: Histogram of Total Cumulative Degradation in 5 Years using 10,000 Simulated Degradation Paths for Fort Peck, MT.

We next calculate the mean and variance of the five-year cumulative degradation at Fort Peck according to the limiting distribution given in (6). For AR(5) with  $\Phi = (0.494, -0.0246, 0.0524, -0.00441, 0.0678)$ ,  $\sum_{i=1}^{365} b_i = 6.018$  and  $(\sum_{i=1}^{365} a_i^2)V = 0.1634$ . These translate to a mean and a standard deviation of five-year cumulative degradation of  $6.018 \times 5 = 30.09$  and  $\sqrt{0.1634 \times 5} = 0.904$ . These numbers are in good agreement with the mean and standard deviation from the histogram, which are 30.08 and 0.908, respectively.

Figure 15 depicts the histogram of failure time at the failure level  $a = 50\%$  for Fort Peck. Comparing with the histogram for Boulder given in Figure 10, two major differences are apparent. First, there is a bimodal distribution for the failure time at Fort Peck, with

one mode much smaller than the other, and second, it takes more time for failure to occur in Fort Peck than in Boulder (most of the distributional mass for Boulder lies between 1950 and 2080 days, whereas for Fort Peck most of the distribution is between 2800 and 3200 days). Fort Peck has a longer life distribution because there is, on average, less UV radiation and lower temperature at the higher latitude of its location, resulting in slower degradation rate.

The bimodality in Figure 15 is caused by the nearly zero slopes of the degradation paths during winter time. This can be best explained by looking at the plot in Figure 16. The failure times in the plot occur when the paths intersect the degradation line at 50% (the failure level). The smaller clump of failure times arise from the fact some of the degradation paths cross the failure line early before the winter sets in. During the winter the degradation paths that are still below the failure level move almost in parallel to the horizontal line because of the slow degradation rate. Very few degradation paths cross the failure level during this time. This is reflected in the histogram by the near absence of failure times between 2880 and 2960 days. After winter, the slopes of the paths increase, and the yet-to-fail paths eventually cross the failure level at 50% , giving rise to the second and larger clump of failure times in the histogram.

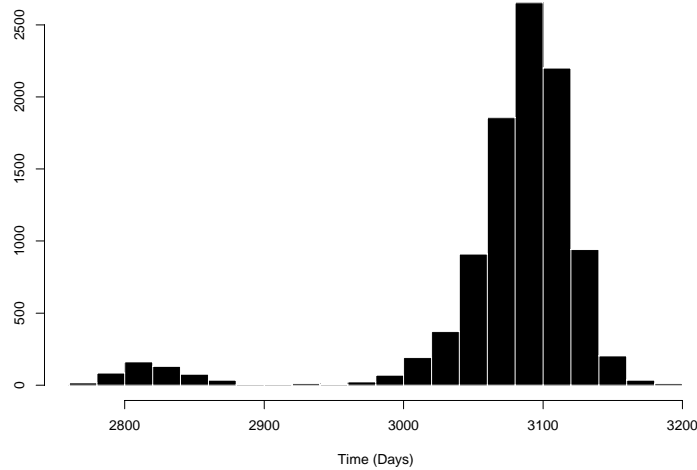


Figure 15: Histogram of Simulated Failure Times for Fort Peck, MT with a Failure Level at 50%, based on 10,000 Simulated Degradation Paths.

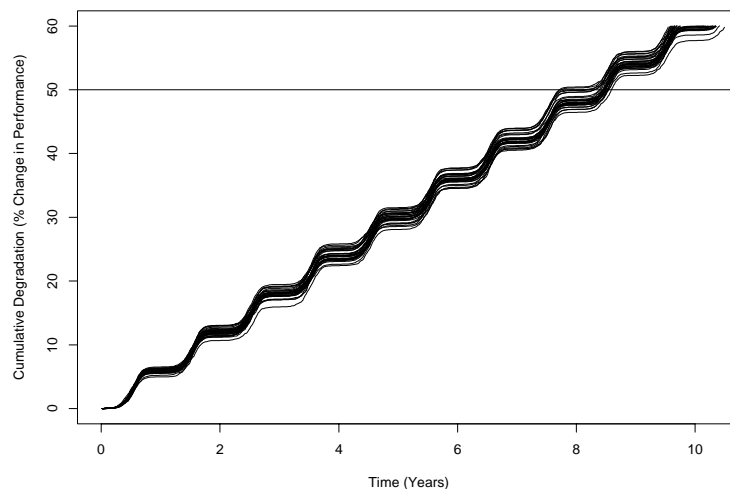


Figure 16: Thirty Simulated Degradation Paths from Time Series Modeling of Daily Degradation for Fort Peck, MT with Failure Level at 50%.

## 6 Concluding Remarks and Areas of Future Research

In this paper, we have presented and illustrated a method to estimate degradation reliability measures for degradation processes induced by exposure to outdoor environments. The method provides an easier alternative to the more challenging task of developing a parametric model for the joint behavior of environmental variables.

Our method requires only an adequate parametric model for the daily degradation, which is univariate. Obtaining such a model may, however, be difficult, especially in applications with complicated chemical reactions with more than one rate constant. The data for daily degradation, estimated or observed, may consist of multiple types of degradation. For example, the degradation rate of a weathering-degradable material may depend on the presence of water or snow on its surface. The degradation data of such material may be more difficult to characterize using a univariate time series model, the approach which we use in this paper. It may involve, for example, determining separate models depending on the presence and the type of precipitation present on the degrading material.

There is, however, a nonparametric method that can handle such situations. Bootstrap

methods can be used to directly resample from the daily degradation data to estimate the degradation and failure time distributions. These methods do not require a search for a model and do not depend on the nature of the daily degradation data. They do, nevertheless, have some implementation issues that need to be addressed before they can be used, namely using blocks of data for resampling and determining the block size. These methods are under investigation.

Another outgrowth of the work presented in this paper that we are currently working on is the extension of the degradation model to include random parameters  $\boldsymbol{\theta}$  that would allow for unit-to-unit or batch-to-batch variability. The presence of two random sources of variability,  $\Psi(t)$  and  $\boldsymbol{\theta}$ , will induce new reliability measures and interpretations.

Other related areas worthy of future investigation include the distribution of cumulative degradation as a mixture of different environments, and as a mixture of multiple batches of products introduced into the service environment at different times.

## 7 Appendix A

### Derivation of the Limiting Distribution of $D(t; \Psi[0, t], \boldsymbol{\theta})$

We first quote Theorem 6.3.4 on page 329, Fuller (1996):

**Theorem 1** *Let  $\{X_t : t \in T = (0, \pm 1, \pm 2, \dots)\}$  be a time series defined by*

$$X_t = \sum_{j=0}^{\infty} \alpha_j e_{t-j},$$

where  $\sum_{j=0}^{\infty} |\alpha_j| < \infty$ , and the  $e_j$  are independent  $(0, \sigma^2)$  random variables with distribution functions  $F_t(e)$  such that

$$\lim_{\delta \rightarrow \infty} \sup_{t \in T} \int_{|e| > \delta} e^2 dF_t(e) = 0.$$

Let  $\{C_t\}_{t=1}^{\infty}$  be a sequence of real numbers satisfying the following conditions:

1.  $\lim_{n \rightarrow \infty} \sum_{t=1}^n C_t^2 = \infty$ ,
2.  $\lim_{n \rightarrow \infty} C_n^2 / (\sum_{t=1}^n C_t^2) = 0$ ,
3.  $\lim_{n \rightarrow \infty} (\sum_{t=1}^n C_t^2)^{-1} \sum_{t=1}^{n-h} C_t C_{t+|h|} \equiv g(h)$ ,  $h = 0, \pm 1, \pm 2, \dots$

Define  $V = \sum_{h=-\infty}^{\infty} g(h) \gamma_X(h) \neq 0$ , where  $\gamma_X(h)$  is the autocovariance function of  $X$  at lag  $h$ . Then

$$\left( \sum_{t=1}^n C_t^2 \right)^{-1/2} \sum_{t=1}^n C_t X_t \xrightarrow{d} N(0, V).$$

□

An autoregressive model of order  $p$ ,  $\text{AR}(p)$ , i.e.,

$$X_i = \phi_1 X_{i-1} + \phi_2 X_{i-2} + \dots + \phi_p X_{i-p} + \epsilon_i,$$

that has independent and normal errors  $\epsilon_i$  satisfies the hypotheses of Theorem 1. The sequence  $a_i$ ,  $i = 1, 2, \dots$ , defined in Section 3.1 meets Conditions 1 and 2. The function  $g(h)$  in Condition 3 is obtained by the following theorem:

**Theorem 2** Let  $\{a_t\}_{t=1}^{\infty}$  be a sequence of nonnegative real numbers, not all zeros, with period  $\tau$ , i.e.,  $a_{t+s\tau} = a_t$  for all  $t$  and  $s \in \mathbf{N}$ . Define

$$g_n(h) = \frac{\sum_{t=1}^{n+mh} a_t a_{t+|h|}}{\sum_{t=1}^n a_t^2}$$

where  $m, h \in \mathbf{Z}$ . Then

$$g(h) \equiv \lim_{n \rightarrow \infty} g_n(h) = \frac{\sum_{t=1}^{\tau} a_t a_{t+|h|}}{\sum_{t=1}^{\tau} a_t^2}.$$

**Proof** Without loss of generality, let  $0 < |mh| < n$ . Then

$$\frac{\sum_{t=1}^{n+mh} a_t a_{t+|h|}}{\sum_{t=1}^n a_t^2} = \frac{\sum_{t=1}^n a_t a_{t+|h|}}{\sum_{t=1}^n a_t^2} + \frac{K}{\sum_{t=1}^n a_t^2}$$

where  $K$  is equal to  $-\sum_{t=n+mh+1}^n a_t a_{t+|h|}$  when  $mh < 0$  and  $\sum_{t=n+1}^{n+mh} a_t a_{t+|h|}$  when  $mh > 0$ . But  $|K| \leq |mh| \max_{1 \leq t \leq \tau} \{a_t a_{t+|h|}\}$ , so the second term vanishes as  $n \rightarrow \infty$ . Now note that for any  $n$

$$\frac{\sum_{t=1}^n a_t a_{t+|h|}}{\sum_{t=1}^n a_t^2} = \frac{k \sum_{t=1}^{\tau} a_t a_{t+|h|} - \delta_1}{k \sum_{t=1}^{\tau} a_t^2 - \delta_2}$$

where  $k = \lceil n/\tau \rceil$  and  $0 \leq \delta_1 < \sum_{t=1}^{\tau} a_t a_{t+|h|}$ ,  $0 \leq \delta_2 < \sum_{t=1}^{\tau} a_t^2$ . Therefore, as  $n \rightarrow \infty$ ,  $k \rightarrow \infty$  and so

$$g(h) = \frac{\sum_{t=1}^{\tau} a_t a_{t+|h|}}{\sum_{t=1}^{\tau} a_t^2}.$$

□

Note that  $g(h)$  is periodic with the same period as  $a_i$  and is an even function with respect to integer arguments. Thus, we can write  $V = \sum_{h=-\infty}^{\infty} g(h) \gamma_X(h) = g(0) \gamma_X(0) + 2 \sum_{h=1}^{\infty} g(h) \gamma_X(h)$ , where  $\gamma_X(h)$  is the autocovariance function for time series  $X_t$ . For a stationary  $\text{AR}(p)$  model,  $\gamma_X(h)$  is infinitely summable, and since  $g(h)$  is bounded, the infinite sum in the expression for  $V$  is convergent. To compute  $V$ , we need to obtain the

autocovariance function  $\gamma_X(h)$  explicitly. For an AR( $p$ ) model, this entails solving the Yule-Walker equations:

$$\begin{aligned}\gamma(0) - \phi_1\gamma(1) - \dots - \phi_p\gamma(p) &= \sigma^2 \\ \gamma(h) - \phi_1\gamma(h-1) - \dots - \phi_p\gamma(h-p) &= 0, \quad h = 1, 2, \dots,\end{aligned}$$

where  $\sigma^2$  is the variance of the error term in the AR( $p$ ) model, and we have dropped the  $X$  subscript for convenience. The solution to the Yule-Walker equations is readily available in numerous time series softwares.

Thus, by Theorem 1,

$$\frac{\sum_{t=1}^n a_t X_t}{\sqrt{\sum_{t=1}^n a_t^2}} \xrightarrow{d} N(0, V).$$

Since for  $t = n$  days,  $D(t; \Psi[0, t], \boldsymbol{\theta}) = D_0 + \sum_{i=1}^n W_i = D_0 + \sum_{i=1}^n b_i + \sum_{i=1}^n a_i X_i$ , we have thus derived the expression in (6).

## References

- Bauer, D. R., and Martin, J. W., Editors (1999), *Service Life Prediction of Organic Coatings, A Systems Approach*, American Chemical Society: Washington.
- Bauer, D. R., and Martin, J. W., Editors (2001), *Service Life Prediction: Methodologies and Metrologies*, Bauer, D. R., and Martin, J. W., Editors, American Chemical Society: Washington.
- Bogdanoff, J. L., and Kozin, F. (1985), *Probabilistic Models of Cumulative Damage*, John Wiley: New York.
- Brockwell, P. J., and Davis, R. A. (1996), *Introduction to Time Series and Forecasting*, Springer-Verlag: New York.
- Eyring, H., Gladstones, S., and Laidler, K. J. (1941), *The Theory of Rate Processes*, McGraw Hill: New York.
- Fuller, W. A. (1996), *Introduction to Statistical Time Series*, 2nd. Edition, Wiley: New York.
- Gertsbakh, I. B., and Kordonsky, K. B. (1969), *Models of Failure*, English translation from the Russian version, Springer-Verlag: New York.
- Gillen, K.T., and Celina, M. (2001), "The Wear-out Approach for Predicting the Remaining Lifetime of Materials", *Polymer Degradation and Stability*, **71**, 15-30.

- Jorgensen, G. J., Kim, H. M., and Wendelin, T. J. (1996), "Durability Studies of Solar Reflector Materials Exposed to Environmental Stresses", *Durability Testing of Non-metallic Materials, ASTM STP 1294*, Herling, R. J., Editor, American Society for Testing and Materials.
- Martin, J. W., (1999), "A Systems Approach to the Service Life Prediction Problem for Coating Systems", *Service Life Prediction of Organic Coatings, A Systems Approach*, Bauer, D. R., and Martin, J. W., Editors, American Chemical Society: Washington.
- Martin, J. W., Saunders, S. C., Floyd, F. L., and Wineburg, J. P. (1996), "Methodologies for Predicting the Service Lives of Coating Systems", *Federation of Societies for Coatings Technology*, Blue Bell: PA.
- Meeker, W. Q., and Escobar, L. A. (1998), *Statistical Methods for Reliability Data*, Wiley: New York.
- Meeker, W. Q., Escobar, L. A., and Chan, V. (2001), "Using Accelerated Tests to Predict Service Life in Highly Variable Environments", *Service Life Prediction: Methodologies and Metrologies*, Bauer, D. R., and Martin, J. W., Editors, American Chemical Society: Washington.
- Meeker, W. Q., Escobar, L. A., and Lu, C. J. (1998), "Accelerated Degradation Tests: Modeling and Analysis", *Technometrics*, **40**, 89-99.
- Meeker, W. Q., and LuValle, M. J. (1995), "An Accelerated Life Test Model based on Reliability Kinetics", *Technometrics*, **37**, 133-146.
- Nelson, W. (1990), *Accelerated Testing: Statistical Models, Test Plans, and Data Analysis*, Wiley: New York.
- Nelson, W. (2001), "Prediction of Field Reliability of Units, Each under Differing Dynamic Stresses, from Accelerated Test Data", *Advances in Reliability*, Rao, C. R., and Balakrishnan, N., Editors, Elsevier Science: Amsterdam.
- Pearce, W. T. et al. (1954), *ASTM STP 1294*, American Society for Testing and Materials.
- Pickett, J. and Gardner, M. (2001), "Effect of Environmental Variables on the Weathering of Engineering Thermoplastics", Preprint.
- Saunders, S. C. (1970), "A Probabilistic Interpretation of Miner's Rule. II", *Journal of Applied Mathematics*, **19**, 251-265.
- Saunders, S. C. (1982), "Cumulative Damage Models", *Encyclopedia of Statistical Sciences*, Kotz, S., and Johnson, N. L., Editors, **2**, 230-233.

Singpurwalla, N. D. (1995), "Survival in Dynamic Environments", *Statistical Science*, **10**, 86-103.

Tobias, P. A., and Trindade, D. C. (1995), *Applied Reliability*, 2nd Edition, Van Nostrand Reinhold: New York.